ARTICLE
Journal of Cellular Biochemistry 108:315–325 (2009)

Journal of Cellular Biochemistry

DNA Methylation and Histone Modification Regulate Silencing of OPG During Tumor Progression

Tung-Ying Lu,[1,2] Cheng-Fu Kao,[1] Chin-Tarng Lin,[2] Dah-Yeou Huang,[2] Chien-Yu Chiu,[1] Yu-Shin Huang,[1] and Han-Chung Wu[1,2*]

[1]*Institute of Cellular and Organismic Biology, Academia Sinica, Taipei 115, Taiwan*

[2]*Institute of Pathology, National Taiwan University, Taipei 100, Taiwan*

ABSTRACT

The identification of molecules that are down-regulated in malignant phenotype is important for understanding tumor biology and their role in tumor suppression. We compared the expression profile of four normal nasal mucosal (NNM) epithelia and a series of nasopharyngeal cancinoma (NPC) cell lines using cDNA microarray and confirmed the actual expression of the selected genes, and found osteoprotegerin (OPG) to be ubiquitously deficient in NPC cells. We also found OPG to be down-regulated in various cancer cell lines, including oral, cervical, ovarian, lung, breast, pancreas, colon, renal, prostate cancer, and hepatoma. Administration of recombinant OPG (rOPG) brought about a reduction in cancer cell growth through apoptotic mechanism. We generated eleven monoclonal antibodies (MAbs) against OPG to study OPG's expression and biological functions in cancer cells. OPG was detected in the tumor stromal regions, but not in the cancer cell per se in surgical specimens of liver cancer. Quantitative reverse transcription-polymerase chain reaction (Q-RT-PCR) revealed that OPG was down-regulated in NPC tissues compared with normal nasal polyp (NNP) tissues. In addition, we showed OPG silencing to be associated with promoter methylation as well as histone modifications. In OPG-silenced cancer cell lines, the OPG gene promoter CpG dinucleotides were highly methylated. Compared to normal cells, silenced OPG gene in cancer cells were found to have reduced histone 3 lysine 4 tri-methylation (H3K4me3) and increased histone 3 lysine 27 tri-methylation (H3K27me3). Taken together, these results suggest that OPG silencing in carcinoma cancer cells occurs through epigenetic repression. J. Cell. Biochem. 108: 315–325, 2009.

KEY WORDS: NASOPHARYNGEAL CARCINOMA; OPG; TUMOR PROGRESSION; EPIGENETIC SILENCING

Carcinogenesis is a multistep process involving multiple genetic events. In this process, cancer cells benefit from the imbalance of oncogenes and tumor-suppressor genes by acquiring preferential growth ability. It is important to identify molecules that are particularly repressed in cancer cells to understand tumorigenesis and to develop new therapeutic strategies as well. Using cDNA microarray to compare genes from NPC and NNM cells, we found NNM cells to have a ubiquitous sevenfold or more OPG (TNFRSF11b) expression than NPC cells. Therefore, we further investigated the biological function, gene regulation, and clinicopathological significance of this protein.

The tumor necrosis factor receptor (TNFR) superfamily members are thought to influence the immune system by modulating innate and adaptive immunity as well as inducing tumor cell cytotoxicity and programmed cell death. OPG, a soluble member of the TNFR superfamily [Ashkenazi, 2002], encodes a protein of 401 amino acids with four N-terminal cysteine-rich domains which is structurally similar to the extracellular domain of other TNFR members and two C-terminal death domain homologue (DDH) regions. This means it may potential induce cell apoptosis [Yamaguchi et al., 1998]. OPG was originally characterized as having a role in bone homeostasis through the suppression of osteoclast formation and function [Simonet et al., 1997]. OPG acts as a decoy receptor. It inhibits osteoclastogenesis by binding to receptor activator of nuclear factor-κB ligand (RANKL) and prevents RANKL communicating with its receptor activator nuclear factor-κB (RANK) on the osteoclast precursors to maturation and bone resorption [Lacey et al., 1998; Yasuda et al., 1998; Kong et al., 1999].

Tung-Ying Lu and Cheng-Fu Kao contributed equally to this work.

Additional Supporting Information may be found in the online version of this article.

Grant sponsor: Academia Sinica; Grant sponsor: National Science Council, Taiwan; Grant number: NSC-96-2323-B-001-002.

*Correspondence to: Dr. Han-Chung Wu, PhD, Institute of Cellular and Organismic Biology, Academia Sinica, 128 Academia Road, Section 2, Nankang, Taipei 11529, Taiwan. E-mail: hcw0928@gate.sinica.edu.tw

Received 3 December 2008; Accepted 29 May 2009 • DOI 10.1002/jcb.22256 • © 2009 Wiley-Liss, Inc.

Published online 29 June 2009 in Wiley InterScience (www.interscience.wiley.com).

Previous studies of OPG being delivered as a recombinant protein (Fc-OPG) have shown it to inhibit the formation of osteoclast in vitro and in vivo and prevent osteolysis in models of cancer-induced bone loss [Capparelli et al., 2000; Croucher et al., 2001; Zhang et al., 2001]; however, its expression and function in cancer cells has not been studied.

Cancer is thought to be a disease of the DNA. Both genetic and epigenetic lesions are thought to contribute to alterations in gene expression. DNA hypermethylation and histone modification have been found to bring about epigenetic changes on promoters of tumor suppressor genes (TSG), causing severe gene repression and a loss of function [Baylin and Ohm, 2006; Esteller, 2007]. Epigenetic events such as DNA methylation, histone modification, and chromatin remodeling result in chromatin structure changes and are involved in the transcriptional silencing of TSG [Baylin and Ohm, 2006; Esteller, 2007]. DNA hypermethylation frequently occurs with appearance of methyl-cytosine-binding proteins (MBPs) on methylated cytosines within various chromatin-remodeling complexes. MBPs like MeCP2 and MBD2 recruit transcriptional corepressors which are known to interact with histone deacetylase (HDAC) [Esteller, 2007]. Although evidence supports that DNA hypermethylation renders local changes in histone modification that synergistically results in a gene silent state, the relevance of histone modifications and DNA methylation in the regulation of the OPG gene expression is still not understood.

To clarify the biological significance of OPG in tumor progression, we examined OPG expression in a series of NNMs, NPCs, and other cancer cells. We also found OPG expression to be detected only in the stromal region of tumor tissues but was silenced in cancer cells from specimens of cancer patients. The repressed expression of OPG may be mainly a consequence of DNA methylation and histone modification. Together, these data suggest that OPG may suppress the proliferation of cancer cells and that its epigenetic down-regulation of OPG may contribute tumor progression.

MATERIALS AND METHODS

CELL CULTURE AND CHEMICALS

Human cell lines were used as follows: nasopharyngeal carcinoma (NPC-TW01–10, NPC-CGBM1, HONE-1, CNE-1 and CNE-2), oral cancer (Ca9-22 and SAS), cervical cancer (Caski and HeLa), ovarian cancer (SKOV-3), lung cancer (CL1-5, H441, H460 and H520), breast cancer (BT483, HBL435 and MDA-MB231), pancreatic cancer (MIA PaCa-2), colorectal cancer (COLO 205, HCT116 and SW620), hepatocellular carcinoma (Hep3B and Mahlavu), renal cell carinoma (A498), prostate cancer (PC3), and primary culture of normal nasal mucosal epithelia (NNM1–4). NPC-TW01–10 were established in our laboratory [Lin et al., 1990, 1993]. NPC-CGBM1 was a gift from Dr. Shuen-Kuei Liao (Chang-Gung University, Linkou, Taiwan). HONE-1, CNE-1, and CNE-2 were established in mainland China. CL1-5 has been described previously [Chu et al., 1997]. Hep3B and Mahlavu were obtained courtesy of Dr. Michael Hsiao (Genomic Research Center, Academia Sinica). Other cell lines were purchased from the American Type Culture Collection (Manassas, VA). All cell lines were grown in DMEM containing 5% FCS under a humidified atmosphere of 95% air and 5% CO_2 except CL1-5, H460 and PC3 in RPMI 1640, MDA-MB231 in F12/DMEM (Gibco-BRL, Grand Island, NY). Native rOPG expressed by mammalian cells was purchased from R&D Systems (185-OS-025; R&D Systems, Minneapolis, MN).

RNA EXTRACTION AND SEMI-QUANTITATIVE/QUANTITATIVE REAL-TIME RT-PCR

RNA was extracted from the cell lines using ULTRASPEC RNA isolation reagent (Biotecx Laboratories, Houston, TX), and cDNA was reverse transcribed with oligo(dT) primer (Fermentas, Glen Burnie, MD) from 4 μg of total RNA using SuperScript III reverse transcriptase (Invitrogen, Carlsbad, CA) according to the manufacturer's instructions. Thirty cycles of RT-PCR were done at 95, 55, and 72°C for 1 min for OPG-specific primers as described in Supplementary Table SI.

For tissue-based expression analysis, primary NNP tissues were a gift from Dr. Pei-Jen Lou (Department of Otolaryngology, National Taiwan University Hospital, Taipei, Taiwan) and NPC tissues were obtained from the archives of the Department of Pathology, National Taiwan University Hospital, Taipei, Taiwan. Total RNA of tissues was extracted using the RNeasy Mini isolation kit (Qiagen, Valencia, CA) following the vendor's protocol. The OPG-specific primers for Q-RT-PCR were used as described in Supplementary Table SI. The use of human specimens in this research was approved by the Institutional Review Board in the National Taiwan University Hospital.

CLONING, EXPRESSION, AND PURIFICATION OF rOPG

Total RNA from NNM cells was used for cloning of human OPG. Human OPG vector was constructed by RT-PCR using primer pairs as listed in Supplementary Table SI. PCR was performed using thirty cycles of 95°C for 30 s, the annealing temperature 56°C for 30 s, and 72°C for 1 min followed by a final extension at 72°C for 10 min. The gene fragment of mature OPG from amino acid sequence 22-401 [Simonet et al., 1997] was cloned into the expression vector pET151/D-TOPO (Invitrogen) and transformed into *E. coli* strain BL21(DE3) pLysS (Invitrogen). For expression of recombinant proteins, cells were grown to an OD600 value of 0.6, induced with 1 mM isopropyl-D-thiogalactoside, and harvested after 2 h at 37°C. Recombinant OPG was purified using Ni-NTA agarose resin (Amersham Pharmacia Biotech, Piscataway, NJ). The purified protein was further confirmed by mass spectrometry. To remove endotoxin from the recombinant proteins, Triton X-114 (Sigma–Aldrich, St. Louis, MO) was added to the protein preparation to a final concentration of 1%. The mixture was incubated at 4°C for 30 min, transferred to 37°C for 10 min, and centrifuged (20,000*g*, 10 min) at 25°C. The upper aqueous phase containing the recombinant protein was carefully removed and purified by Triton X-114 preparation for two more cycles.

PLASMID PREPARATION AND TRANSFECTION

The coding region of human OPG was amplified from cDNA derived from NNM cells, using primers as described in Supplementary Table SI and ligated into pBIG2i [Strathdee et al., 1999]. The pBIG2i vector is a tetracycline-responsive gene expression system and contains a selective marker conferring resistance to hygromycin B for the generation of stable cell lines. Clones containing the OPG insert (pBIG2i-OPG) were sequenced and a 100% matching clone was

transfected into NPC-TW04 and HCT116 cells respectively by Lipofectamine 2000, according to the manufacturer's recommendations (Life Technologies, Rockville, MD). Selection of transfected cells were maintained using 200 μg/ml hygromycin B (Sigma–Aldrich), and OPG expression was induced by adding 0.02–4 μg/ml doxycyclin (Sigma–Aldrich).

CELL PROLIFERATION ASSAY

Cell growth rate was determined by 3-(4,5-dimethyl-2-thiazolyl)-2,5-diphenyl-2H-tetrazolium bromide (MTT, Sigma–Aldrich) assay. Cells were seeded in 96-well plate. At different time points, the cell growth was determined by adding MTT and incubated at 37°C for 2.5 h. The insoluble formazan product formed and was solubilized with DMSO (150 μl/well). The plates were read wavelength of 570 nm by a microtiter plate reader. Furthermore, to verify that the growth inhibitory effect was not due to endotoxin, rOPG was digested with proteinase K (Sigma–Aldrich) for 1 h at 37°C, and then the proteinase K was inactivated by heating for 10 min at 100°C. The experiment was done in triplicate.

TUNEL ASSAY

Terminal deoxynucleotidyl transferase-mediated deoxynucleotide triphosphate nick end-labeling (TUNEL) was used to evaluate in situ apoptosis in tumor cells. NPC-TW04 cells were seeded into 24-well chamber slides and incubated with 10 μg/ml of rOPG or BSA separately for 48 h. The cells were then stained with in situ cell death detection reagent (Roche Molecular Biochemicals, Indianapolis, IN) according to the manufacturers' instructions. The nuclei were counterstained with 4,6-diamidino-2-phenylindole (DAPI; blue fluorescence), and TUNEL-positive cells were visualized under the fluorescence microscope.

GENERATION OF MAbs AGAINST HUMAN OPG

The production of MAbs against OPG was generated according to a standard procedure [Kohler and Milstein, 1975] with some modifications [Wu et al., 2003; Chen et al., 2007]. Briefly, female BALB/c mice were immunized intraperitoneally with purified rOPG four times at 3-week intervals. On day 4 after the final boost, lymphocytes of the immunized mouse spleen were fused with NSI/1-Ag4-1 myeloma cells, using 50% (vol/vol) polyethylene glycol (Gibco-BRL). The fused cell pellet was resuspended in DMEM supplemented with 20% FCS, hypoxanthine-aminopterin-thymidine (HAT) medium, and hybridoma cloning factor (ICN Biomedicals, Aurora, OH). Hybridoma supernatants that bound rOPG were screened by ELISA. Selected candidate clones were further subcloned by limiting dilution. Ascitic fluids were produced in pristane-primed BALB/c mice. Hybridoma cell lines were grown in DMEM with 10% FCS. Final hybridoma clones were isotyped using an isotyping kit from Southern Biotech (Southern Biotech, Birmingham, AL) according to the manufacturer's instructions. MAbs were affinity purified with protein G sepharose gel (Amersham Pharmacia Biotech). ELISA and Western blotting were used to measure the activity and specificity of antibodies.

SCREENING OF MAbs AGAINST OPG BY ELISA

ELISA plates (Corning Costar, St. Louis, MO) were coated overnight at 4°C with purified rOPG (10 μg/ml) in 0.1 M bicarbonate buffer, pH 8.6. The plates were subjected to blocking with 1% BSA in phosphate-buffered saline (PBS). MAbs against OPG were added to the plates of rOPG and incubated at room temperature for 1 h. The plates were washed three times with PBS containing 0.1% (w/v) Tween-20 (PBST0.1) and incubated with horseradish peroxidase (HRP)-conjugated anti-mouse immunoglobulin G (IgG) (Jackson ImmunoResearch Laboratories, West Grove, PA) for another 1 h. The plates were washed five times with PBST0.1 and incubated with the peroxidase substrate *o*-phenylenediamine dihydrochloride (OPD, Sigma–Aldrich). The reaction was stopped with 3 N HCl, and the plates were read using a microplate reader at 490 nm.

WESTERN BLOT ANALYSIS

Proteins were extracted with RIPA buffer (150 mM NaCl, 1.0% Nonidet P-40, 0.5% sodium deoxycholate, 0.1% SDS, 50 mM Tris–HCl, pH 7.4) plus proteinase inhibitor (Roche), separated by 10% sodium dodecyl sulfate–polyacrylamide gel electrophoresis (SDS–PAGE), and transferred to a nitrocellulose membrane (Hybond-C Super; Amersham, Little Chalfont, UK). The membranes were incubated with anti-OPG (1:500; OPG38-5 ascitic fluids) or anti-α-tubulin (1:10,000; Sigma–Aldrich) MAbs, and subsequently incubated with HRP-conjugated goat anti-mouse IgG (Jackson ImmunoResearch Laboratories). The signals were detected using chemiluminescence reagents (ECL; Amersham).

IMMUNOPRECIPITATION

Serum-free conditioned media (0.5 ml) obtained from 2-day cultured NNM cells were incubated with anti-OPG MAbs for 1 h at 4°C. Protein G sepharose gel (Amersham Pharmacia Biotech) was then added to the immune complexes for another 1 h incubation. The complexes were washed with PBST0.1, and extracted by adding sample buffer (Bio-Rad Laboratories, Richmond, CA). The complexes were subsequently heated at 95°C for 5 min, and then the same procedure was used in the section of describing method for "Western Blot Analysis."

SPECIMENS AND IMMUNOHISTOCHEMISTRY

Hepatocellular carcinoma specimens were obtained from the tissue bank of National Taiwan University Hospital (NTUH) with approval from the Institutional Review Board in NTUH. After deparaffinization, the sections were treated with MAb OPG23-1 and normal mouse IgG (NM-IgG) for 1 h at room temperature. Following washing in PBST0.1, a biotin-free super sensitive polymer-HRP detection system (Biogenex, San Ramon, CA) was used to detect immunoreactivity. The slides were subjected to routine immunohistochemical staining [Lee et al., 2007; Lo et al., 2008]. The preparations were lightly counterstained with hematoxylin, mounted with Aquatex (Merck, Dannstadt, Germany), and examined by light microscopy.

PROMOTER METHYLATION EVALUATION

The promoter methylation assay of the OPG gene was performed using a commercial promoter methylation PCR kit (Panomics,

Redwood, CA) following the manufacturer's directions. Briefly, 4 μg genomic DNA from NNM, NPC-TW04 and HCT116 were digested by restriction enzyme *Mse*I (New England Biolabs, Hertfordshire, UK) and DNA was purified using DNA purification column. The purified DNA was incubated with MeCP2 for 30 min at 15°C, and the DNA of the complex was eluted by separation column. We reserved the flow-through from separation column as un-bound DNA controls. The promoter methylation level was measured by real-time PCR using the LightCycler480 System (Roche). Amplification primers were the same as those in ChIP assay. The evaluation was expressed by the ratio of the purified bound fraction to unbound DNA of each sample. The PCR was done in triplicate.

DNA EXTRACTION AND BISULFITE MODIFICATION

The CpG methylation status of OPG promoter was evaluated by bisulfite genomic sequencing. The genomic DNA was isolated using the Wizard genomic DNA purification kit (Promega, Madison, WI). Five hundred nanogram of purified DNA was used for bisulfite reaction by EZ DNA methylation kit according to the manufacturer's directions (Zymo Research, Orange, CA). Completely methylated and unmethylated control genomic DNA was purchased from Qiagen. The primers used for the bisulfite PCR amplifications are listed in Supplementary Table SI. Methylation analysis was carried out on the PCR products by direct PCR sequencing and clonal analysis.

CHROMATIN IMMUNOPRECIPITATION AND QUANTITATIVE REAL-TIME PCR

ChIP assays were carried out on 1×10^5 NNM, NPC-TW04 and HCT116 cells. The protein-DNA complexes were crosslinked using 1% formaldehyde, and sonicated to an average size of 250 bp by MISONIX Sonicator 3000. For immunoprecipitations, 2.4 μg anti-H3K4me3 (Abcam, Cambridge, MA) or 5 μg anti-H3K27me3 (Abcam) was used. The antibody was incubated with Protein A beads (Invitrogen) for 2 h and the complex was further incubated with chromatin for another 2 h. No antibody controls were also included for ChIP assay, and no precipitation was observed. The bound fraction was isolated by Protein A beads according to the manufacturer's instructions, and the immune complexes were subsequently subjected to reverse crosslinking. The immunoprecipited DNA was recovered by PCR purification kit (Qiagen) according to the manufacturer's instructions. The amount of DNA target was measured by real-time PCR using the LightCycler480 System (Roche). Amplification primers are listed in Supplementary Table SI. For each sample, PCR analysis was performed in triplicate, and the bound fraction was compared with input DNA of 1×10^4 cells. The results displayed the ratio of immunoprecipitaed DNA to input DNA (IP/Input). To obtain fold enrichment value, we further normalized the IP/Input value to non-specific binding control: HBB (H3K4me3) or ACTB (H3K27me3).

STATISTICAL ANALYSES

Statistical analyses were done using unpaired Student's *t*-tests as appropriate. $P < 0.05$ was considered significant.

RESULTS

EXPRESSION OF OPG IN NNM CELLS, NPC, AND OTHER CANCER CELL LINES

To identify molecules with particular biological significance in tumorigenesis, especially those down-regulated in cancer cells, we selected OPG from approximately 7500 distinct human transcripts of cDNA microarray. NNM cells expressed 7-fold or more OPG than NPC cells (mean fold expression, 18.76 ± 8.16 SD; range, 7.2–25.96) and its transcription was confirmed by semi-quantitative RT-PCR experiments in four NNM primary culture cells and 14 NPC cell lines (Fig. 1A). OPG was detected in all four NNM cells, weakly detected in NPC-TW01, 05–07, and not detectable in the other 12 NPC cell lines (Fig. 1A).

To further confirm the down-regulation of OPG in cancer, we analyzed expression of OPG protein using Western blot (WB) analysis in NPC and in different types of human cancer cell lines. To do this, we generated eleven MAbs against OPG (Fig. 3). Western blot analysis using anti-OPG MAbs (Fig. 3B) revealed a 55-kDa band in NNM cells (Fig. 1B). The OPG detection signal was very weak in H441 (lung cancer), MDA-MB231 (breast cancer), MIA PaCa-2 (pancreatic cancer), SW620 (colorectal cancer), Hep3B and Mahlavu (hepatocellular carcinoma), and PC3 (prostate cancer). It was not detected in eight NPC (NPC-TW01–08), HONE-1 (nasopharyngeal carcinoma) and other cancer cells, including Ca9-22 and SAS (oral cancer), Caski and HeLa (cervical cancer), SKOV-3 (ovarian cancer), CL1-5, H460 and H520 (lung cancer), BT483 and HBL435 (breast cancer), COLO 205 and HCT116 (colorectal cancer), and A498 (renal cell carcinoma) (Fig. 1B). Among the primary cells and cell lines tested, OPG expression was found to be lower in cancer cells than in normal cells at both the mRNA level and the protein level, indicating that OPG was significantly down-regulated in cancer cells.

GROWTH INHIBITORY EFFECT OF rOPG ON CANCER CELLS

We found OPG to be repressed in tumor cells (Fig. 1) raising the possibility that re-expression of OPG might inhibit tumor growth. To clarify the functional role of OPG, we investigated the effect of rOPG on the growth of cancer cells. NPC-TW01 cells were incubated with rOPG of indicated concentrations, and the cell proliferation was verified using MTT assays. As shown in Figure 2A, rOPG reduced cell growth in a dose-dependent manner by day 5. At concentrations of 1 μg/ml, rOPG inhibited cell growth by almost 25%. At 5 μg/ml, it inhibited cell growth by 50%. Ten μg/ml of rOPG inhibited almost all cell growth. We found no inhibition of growth in the control bovine serum albumin-treated cells at any concentration (Fig. 2A).

In addition to NPC-TW01, we tested the effect of rOPG on the growth of other cancer cell lines including NPC-TW04, 07, HCT116, and BT483, and one normal cell NNM obtained from primary culture. Similarly, cell growth was repressed at 10 μg/ml rOPG in all cancer cells we tested, but interestingly, rOPG did not affect the growth of normal NNM cells (Fig. 2B). rOPG appeared to influence the growth of cancer cells, not normal cells.

To confirm that growth inhibited by rOPG and not due to non-protein toxins from *E. coli*, rOPG was digested with proteinase K before it was used to treat cancer cells, with complete digestion

being confirmed by the absence of rOPG on silver-stained SDS–PAGE (data not shown). As shown in Figure 2C, rOPG's ability to inhibit cancer cell growth was lost when digested with proteinase K, confirming that the cell growth inhibition indeed resulted from exertion by rOPG instead of non-protein toxins from *E. coli* [Lin et al., 2006].

To directly evaluate whether OPG caused tumorigenesis under physical conditions, we engineered ectopic expression through stable transduction of both NPC-TW04 and HCT116 cells with a tetracycline-responsive OPG expression vector [Strathdee et al., 1999]. OPG expression was detected by Q-RT-PCR and Western blot analysis, and found to respond to doxycyclin in a dose-dependent manner (Fig. 2D,E). A low concentration of ectopic OPG not affecting growth rate of these cells (Fig. 2F) but high concentration (10 μg/ml) of rOPG markedly inhibiting cancer cell growth (Fig. 2A,B). To further address the biological function of native OPG in cell viability, we treated NPC cells with mammalian cell-expressed OPG [Secchiero et al., 2006] at 1 μg/ml, and found native OPG caused ~65% growth inhibition in these cells (Fig. 2G) as seen in rOPG from *E. coli*. These results were further supported by the TUNEL assay, which specifically indicated that the reduction of cell viability effect was accompanied by the induction of apoptosis in the rOPG-treated cells (Fig. 2H). Overall, these data suggest that OPG at high concentration can inhibit proliferation of cancer cells but not normal cells through induction of apoptosis.

GENERATION AND CHARACTERIZATION OF MAbs AGAINST OPG

To evaluate the expression of the OPG protein in cells, we generated monoclonal antibodies against the protein. We expressed recombinant His-tagged OPG (rOPG) fusion protein in *E. coli* and purified the protein. The rOPG was further confirmed by MALDI-TOF (Supplementary Fig. S1), and used as an antigen to immunize BALB/c mice. After fusing splenocytes from immunized mice with NSI/1-Ag4-1 mouse myeloma cells, a total of 1,527 surviving hybridoma clones were grown and tested for OPG immunoreactivity by ELISA. Sixty-three hybridoma clones had good reactions (designated as positive clones), and were sub-cloned for monoclonal antibodies using the limiting dilution technique (Supplementary Table SII). Finally, we obtained eleven MAbs, including OPG-Ab 6-1, 21-1, 22-1, 23-1, 29-3, 33-1, 34-2, 38-5, 39-2, 40-2, and 42-1 (Table I). These MAbs were found by ELISA to be able to bind with rOPG (Fig. 3A).

We further analyzed the specificity of these MAbs against OPG extracted from NNM cells by Western blot analysis (Fig. 3B). OPG-Ab 6-1, 38-5, and 42-1 showed immunoreactivity to OPG protein, and only OPG-Ab 38-5 showed a single band of 55-kDa (Fig. 3B). The molecular weight of the immunoreactive band correlated well with that of the known OPG protein [Simonet et al., 1997]. To eliminate the possibility that the selected MAbs might react with His-tag or *E. coli* proteins and to investigate whether MAbs could bind to native OPG protein, we performed immunoprecipitation (IP)—Western blot assay. Since OPG is also known to be a secreted protein, we tested the IP of MAbs binding to native OPG from NNM conditioned media. The serum-free supernatants from 2-day cultured NNM cells were used for IP using anti-OPG MAbs. We found that OPG-Ab 23-1, 29-3, 33-1, 38-5, and 39-2 reacted strongly with native OPG, while 21-1, 34-2, and 40-2 reacted moderately to it (Fig. 3C). The production, isotyping and characterization of anti-OPG MAbs are summarized in Table I.

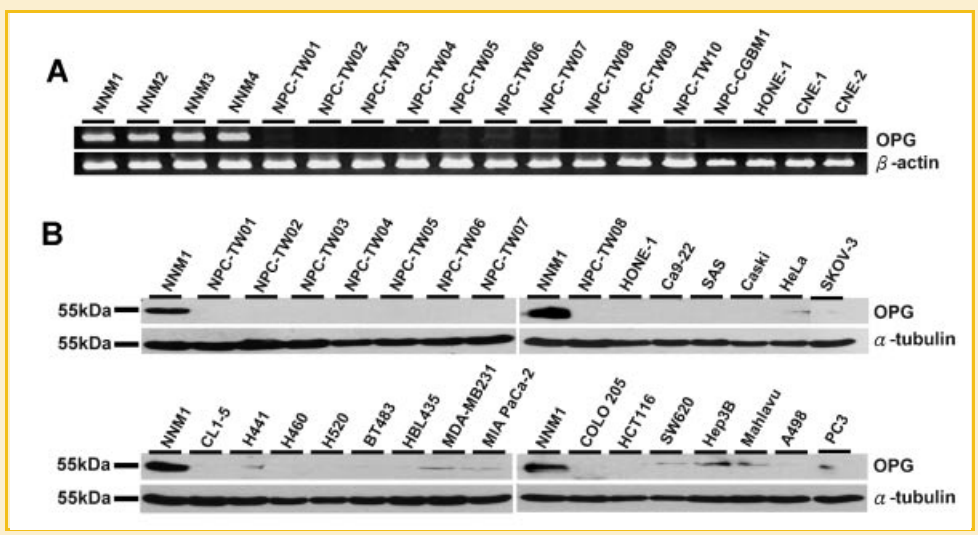

Fig. 1. Expression of OPG in NNM cells, NPC and human cancer cell lines. A: Semi-quantitative RT-PCR was done with the *OPG*-specific primers as described in Materials and Methods Section. Four NNM primary cells and fourteen NPC cells were evaluated. β-Actin gene expression was used as an internal control. B: Expression of the OPG protein was evaluated by Western blot analysis with anti-OPG MAbs. Lysates from NNM (NNM1–4), NPC (NPC-TW01–08 and HONE-1), and other cancer cell lines: oral cancer (Ca9-22 and SAS), cervical cancer (Caski and HeLa), ovarian cancer (SKOV-3), lung cancer (CL1-5, H441, H460 and H520), breast cancer (BT483, HBL435 and MDA-MB231), pancreatic cancer (MIA PaCa-2), colorectal cancer (COLO 205, HCT116 and SW620), hepatoma (Hep3B and Mahlavu), renal cell carcinoma (A498) and prostate cancer (PC3) were collected for Western blot analysis. The band of OPG on 55-kDa was only detected clearly in NNM cells. While some cancer cells such as HeLa, H441, MDA-MB231, MIA PaCa-2, SW620, Hep3B, Mahlavu and PC3 showed trace amounts of OPG, OPG was down-regulated in almost all of the cancer cells. [Color figure can be viewed in the online issue, which is available at www.interscience.wiley.com.]

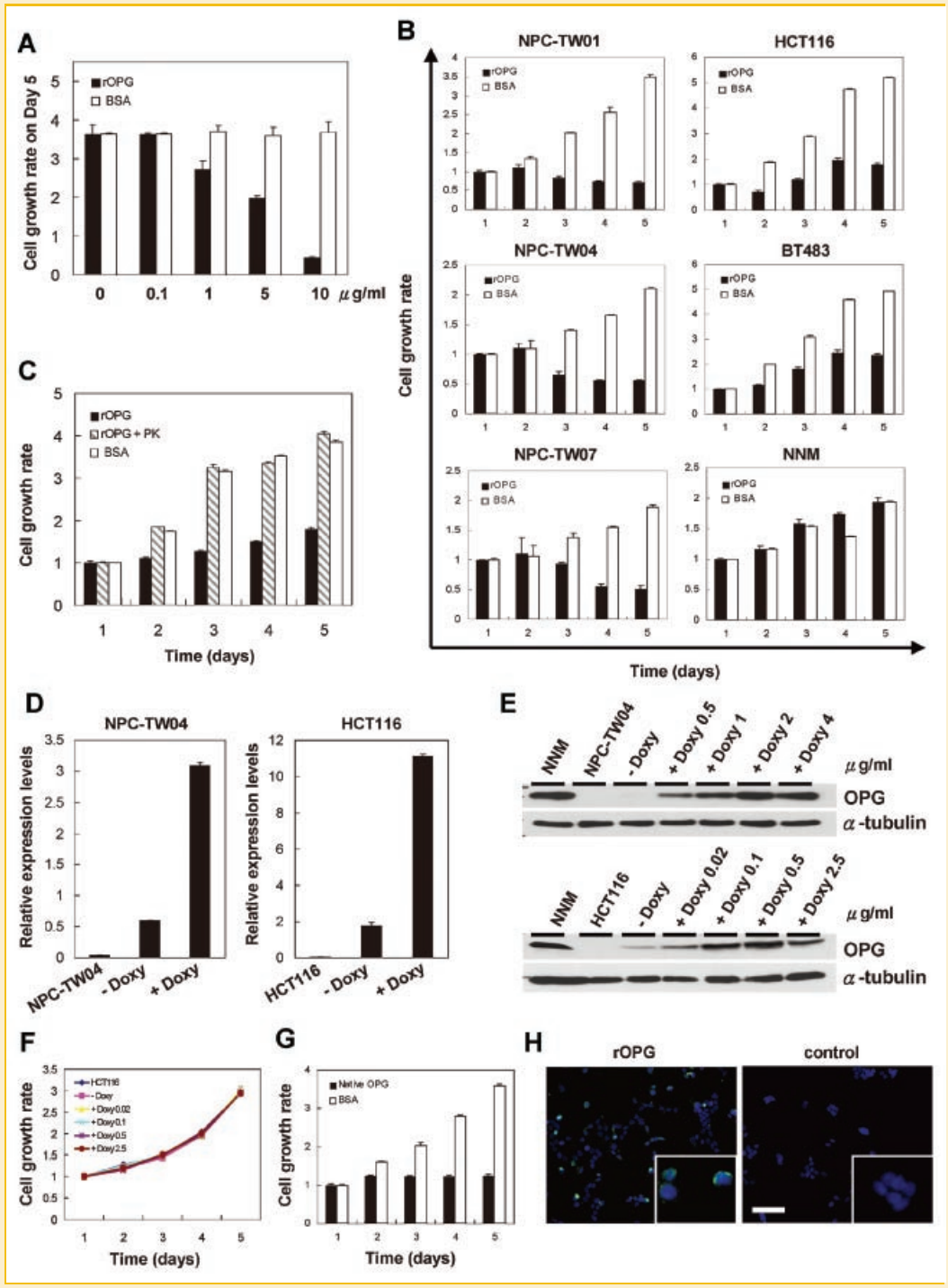

Fig. 2. Recombinant OPG repressed the proliferation of cancer cells. A: NPC-TW01 cells were incubated with indicated concentration of rOPG or BSA, and then MTT assay was used to evaluate cell proliferation. B: 10 μg/ml of rOPG or BSA were incubated with NPC-TW01, NPC-TW04, NPC-TW07, HCT116, BT483, and NNM cells. Cell growth was suppressed by rOPG in cancer cells, but not in NNM cells. C: rOPG was digested with proteinase K (PK) and the mixtures were incubated with HCT116 as described above, and cell proliferation was measured by MTT. D: Q-RT-PCR analysis of OPG mRNA levels in doxycyclin-treated cancer cells. Transfected cells (both OPG-NPC-TW04 and OPG-HCT116) were cultured in the absence or presence of doxycyclin (2 μg/ml) for 48 h. The OPG signal was normalized to the GAPDH signal for analysis, and the parental cells were provided as parallel expression control. Doxycyclin-treated cells had increased expression of OPG mRNA. E: Western blot analysis of OPG levels in conditioned media. OPG immunoreactivity was detected in conditioned media of transfected cells after induction by doxycyclin for 48 h. No or trace OPG was detected in non-induced cells. The corresponding β-actin of each total protein lysate from transfected cells represented loading and internal control. F: Cell proliferation assays. Ectopic expression of OPG after doxycyclin induction (μg/ml) did not alter the proliferation of transfected cells (OPG-HCT116) in vitro. G: NPC-TW04 cells were treated with 1 μg/ml of mammalian cell-expressed native OPG or BSA, and cell viability was assessed by MTT. H: TUNEL assay indicates that rOPG treatment of NPC-TW04 caused apoptosis. Visible apoptotic nuclei were observed in rOPG-treated but not BSA-treated cells (Bar = 100 μm).

TABLE I. Summary of the Main Features of Anti-OPG MAbs

Mab	ELISA	WB	IP	IHC	Isotype
OPG-Ab 6-1	+	+	−	ND	IgM, κ
OPG-Ab 21-1	+	−	+	ND	IgG1, κ
OPG-Ab 22-1	+	−	−	ND	IgA, κ
OPG-Ab 23-1	+	−	+	+	IgG2a, κ
OPG-Ab 29-3	+	−	+	+	IgG1, λ
OPG-Ab 33-1	+	−	+	+	IgG1, κ
OPG-Ab 34-2	+	−	+	ND	IgG1, κ
OPG-Ab 38-5	+	+	+	+	IgG1, κ
OPG-Ab 39-2	+	−	+	+	IgG1, κ
OPG-Ab 40-2	+	−	+	ND	IgG2b, κ
OPG-Ab 42-1	+	+	−	ND	IgM, κ

ND, not determined.

OPG EXPRESSION IN SPECIMENS OF HUMAN TUMOR TISSUES

To expand on our in vitro findings and examine the clinicopathological significance of OPG expression in NPC patients, a real-time Q-RT-PCR assay was performed to detect OPG mRNA in biopsy specimens of NPC. OPG transcript levels were higher in normal nasal polyp tissues (NNP1–NNP5) than in NPC tissues (NPC1–NPC5), though the degree and extent of silencing was not even (Fig. 4A). To further confirm OPG expression was down-regulated in cancer cells, we used immunostaining to detect OPG expression in patients with hepatocellular carcinoma (HCC). Immunoreactivity to OPG was detected in the stromal region of tumor tissues but not in cancer cells themselves (Fig. 4B). Similar results were observed in another four cases (Fig. S2). Control normal mouse IgG (NM-IgG) showed no immunoreactivity (Fig. 4C). Consistent with the in vitro analysis, OPG transcripts and proteins were found to have a significant reduction in cancer cell lines as well as cancer cells in tumor tissues from clinical specimens.

EPIGENETIC REGULATIONS AT THE OPG PROMOTER REGION

The universal suppression of OPG on cancer cells rather than normal ones leads to a fascinating question of whether the down-regulation of *OPG* in cancer may be as a result of hypermethylation in its promoter region. To test the aforementioned rationality, the methylation status on *OPG* promoter was analyzed. MeCP2 is a well-studied member of a family of proteins which can selectively recognize methylated CpGs [Meehan et al., 1992]. Through isolating methylated genomic DNA by MeCP2 binding, we could differentiate methylated from unmethylated promoters. Figure 5A is a representation of the gene structure, primers, and CpG contents encompassed the *OPG* promoter region. As shown in Figure 5B, by examining PCR amplification of MeCP2-binding DNA fragments of NNM, NPC-TW04 and HCT116, we determined promoter methylation status of OPG. In both NPC-TW04 and HCT116 cancer cells, the OPG gene was highly methylated at the upstream or downstream of transcription start site (TSS) (Fig. 5B). We found that the methylation level of upstream of TSS was 9–10-fold higher in cancer cells than in NNM. It was also noticed that the methylation level in HCT116 was 2.5-fold higher in downstream of TSS, while that in NPC-TW04 was 5-fold higher than in NNM cells (Fig. 5B).

To further determine CpG island methylation status of the OPG gene promoter in NNM and tumor cells, we used bisulfite-assisted genomic sequencing. The promoter methylation region was localized on −386 to −43 upstream of TSS. Through clone sequencing, CpG dinucleotides in the OPG promoter were found to be unmethylated in OPG expressing NNM cells. In contrast, the CpG dinucleotides were highly methylated in NPC-TW04 and HCT116 cell lines, two lines in which the OPG gene was silenced (Fig. 5C). These results suggested that the repression of OPG in cancer cell may result from hypermethylation at the promoter.

Previous studies have also suggested that histone tail modifications, including acetylation, methylation, and phosphorylation, correlated with gene activities. Some of them are believed to be activation marks, among which H3K4me3 has been verified to positively correlate with gene expression by serving as anchoring sites for chromatin remodelers or co-activators [Martin and Zhang, 2005]. In contrast, lysine 27 methylation of H3 was found to adversely regulate transcription by promoting a compact chromatin structure. To determine whether the OPG expression level corresponds with these epigenetic events, we performed chromatin

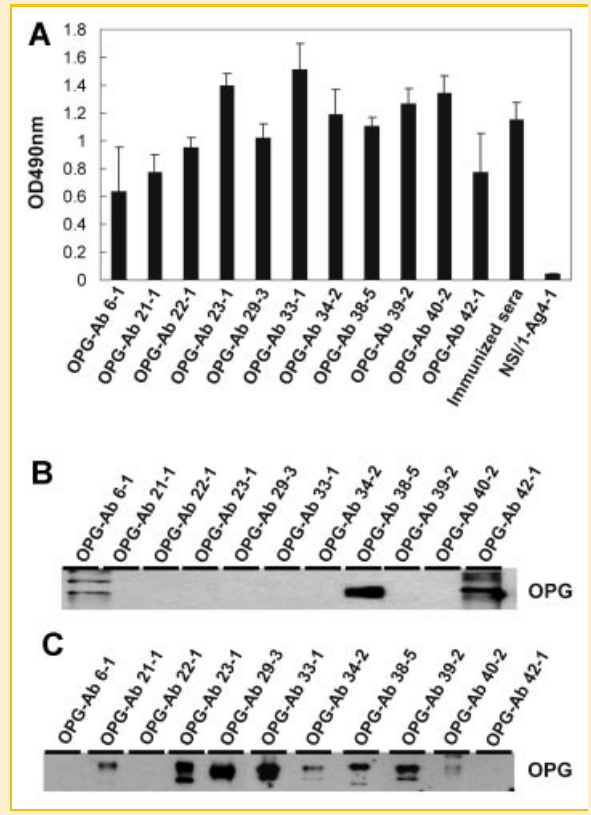

Fig. 3. Generation and characterization of MAbs against human OPG. A: ELISA analyzing binding affinity of the MAbs OPG-Ab 6-1, 21-1, 22-1, 23-1, 29-3, 33-1, 34-2, 38-5, 39-2, 40-2, and 42-1 against rOPG. Supernatants from these MAbs were added onto rOPG-coated ELISA plates. Sera from rOPG hyper-immunized BALB/c mice were used as a positive control, and culture media of NSI/1-Ag4-1 cells was used as a negative control. B: Western blot analysis of the NNM cell lysates with indicated antibodies. MAbs OPG-Ab 6-1, 38-5, and 42-1 recognize human OPG protein using a reducing gel. C: Western blot analysis of immuno-complexes precipitated by indicated anti-OPG MAbs. Protein G sepharose gels were incubated with immuno-complexes of NNM conditioned media plus anti-OPG MAbs. MAbs OPG-Ab 21-1, 23-1, 29-3, 33-1, 34-2, 38-5, 39-2, and 40-2 specifically immunoprecipitate and recognize native OPG proteins. [Color figure can be viewed in the online issue, which is available at www.interscience.wiley.com.]

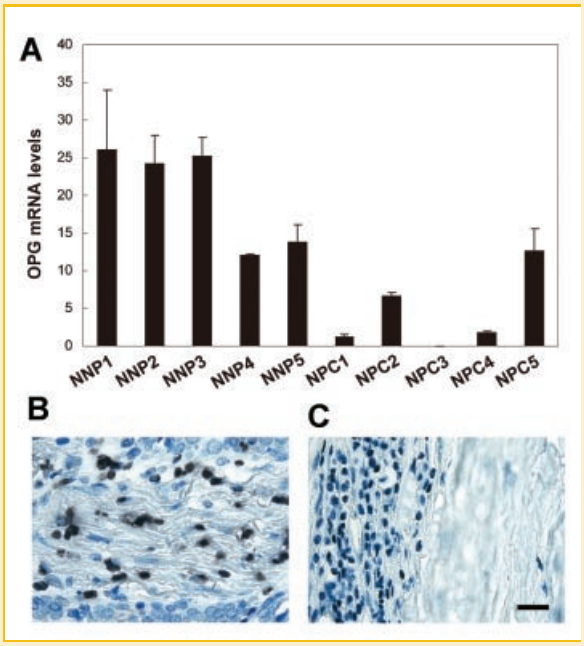

Fig. 4. Identification of OPG expression in normal stromal cells and tumor lesions. A: Real-time PCR quantification was used to detect OPG message levels in five non-cancer nasal polyp (NNP1–NNP5) and in five nasopharyngeal carcinoma (NPC1–NPC5) patients. Four out of five NPC patients showed repressed OPG message levels. B: Immunohistochemical staining of OPG in HCC surgical specimens. Immunoreactivity of OPG was found in the stromal cells. C: No reaction product was identified when using normal mouse IgG (Bar = 50 μm).

immunoprecipitation assays (ChIP) coupled with quantitative PCR to characterize the surrounded *OPG* promoter region. In OPG-expressed NNM cells, the association of the *OPG* gene promoter with H3K4me3 was two- to threefold greater than in NPC-TW04 and HCT116 cells at the downstream of TSS (Fig. 5D), while there was no significant differences at the upstream of TSS among cell lines. Furthermore, we investigated H3K27me3 mark, since it has been suggested that H3K27me3 levels were higher at silent promoters than at active promoters [Barski et al., 2007]. Our results revealed the levels of H3K27me3 to be significantly higher around TSS of OPG in NPC-TW04 and HCT116 cells, which did not express OPG. Downstream of TSS, H3K27me3 signal was four- to fivefold greater in NPC-TW04 and HCT116 than in NNM. It was also twofold greater in NPC-TW04 and HCT116 upstream of TSS (Fig. 5E). Taken together, these results suggest that the silencing of OPG gene in cancer cells might be regulated by epigenetic mechanisms through both DNA methylation and histone modifications.

DISCUSSION

In this study, we used cDNA microarray analysis to compare the gene expression patterns of NPC and NNM epithelia. We identified some differentially expressed gene groups as well as confirmed that there is OPG down-regulation in not only NPC but also in various other cancers (Fig. 1A,B). Down-regulation of OPG in cancer cells were further confirmed by our study of clinical specimens from cancer patients (Fig. 4). From the repressive expression of OPG it might be suggested that it plays a tumor suppressive role in tumorigenesis and progression. Previous studies concerning the expression of OPG in cancer cells are limited. OPG expression in myeloma cells was restricted [Shipman and Croucher, 2003], corresponding to clinical findings that show that patients with myeloma have lower OPG staining of their surgical biopsies [Pearse et al., 2001]. We also found discrepancies of the OPG expression in prostate cancer, since some of them cause osteoblastic phenotypes while others cause osteolytic or mixed phenotypes [Corey et al., 2002]. The phenotype of prostate cancer may correlate to OPG expression and cancer-stromal cells interaction further shifts expression of growth/survival-related genes in cancer and reduces expression of OPG in osteoblasts [Corey et al., 2002; Holen et al., 2002; Fizazi et al., 2003]. The OPG expression level in cancer and normal cells, however, had not been clearly elucidated until this study.

Previous studies on the physiological function of OPG indicated that it serves as a decoy receptor competing with RANK binding to its ligand RANKL, resulting in inhibition of osteoclast maturation and bone remodeling [Simonet et al., 1997]. OPG can inhibit tumor growth specifically in bones especially in cancers that tend toward bone mtastasis, such as prostate and breast cancer, or bone tumor, like multiple myeloma, though OPG itself does not directly restrain tumor growth [Croucher et al., 2001; Zhang et al., 2001; Vanderkerken et al., 2003; Yonou et al., 2003; Corey et al., 2005]. These results suggest that OPG's ability to inhibit the establishment of cancer may be due specifically to factors in the bone microenvironment. However, a more recent study on osteosarcoma shows it is possible that, when delivered as gene therapy, OPG can prevent tumor cell proliferation and alleviate bone resorption [Lamoureux et al., 2007]. We delivered recombinant OPG to cancer cells and observed their proliferation rates. To our surprise, OPG was able to reduce cancer cell proliferation under concentration from 1 to 10 μg/ml without affecting normal cell growth (Fig. 2B). OPG has been shown to dose-dependently inhibit TRAIL-induced cytotoxicity at 0.2–5 μg/ml [Emery et al., 1998], though the effect of OPG toward cell viability has not been discussed. Our findings suggest either that the amount of OPG accumulates in tumor cells to a certain amount to induce apoptosis or that there exists an unidentified receptor specifically on the tumor cell surface, through which signals are transduced to their cellular targets and induced cell apoptosis.

Based on these findings, we endeavored to generate of MAbs specifically against *E. coli* produced human OPG protein and characterize their application in ELISA, WB and IP. With these specific antibodies available, we had the opportunity to gain a better understanding of the molecular basis of OPG in tumorigenesis. Establishing and selecting from 1,527 analyzed clones, we have successfully generated eleven specific OPG MAbs. These clones might be used in several applications in basic research (Figs. 1B, 3, and 4; Table I). Moreover, these antibodies provide new insights to help in the hunt for their potential interacting partners. These OPG antibodies might help us understand the interaction involved in

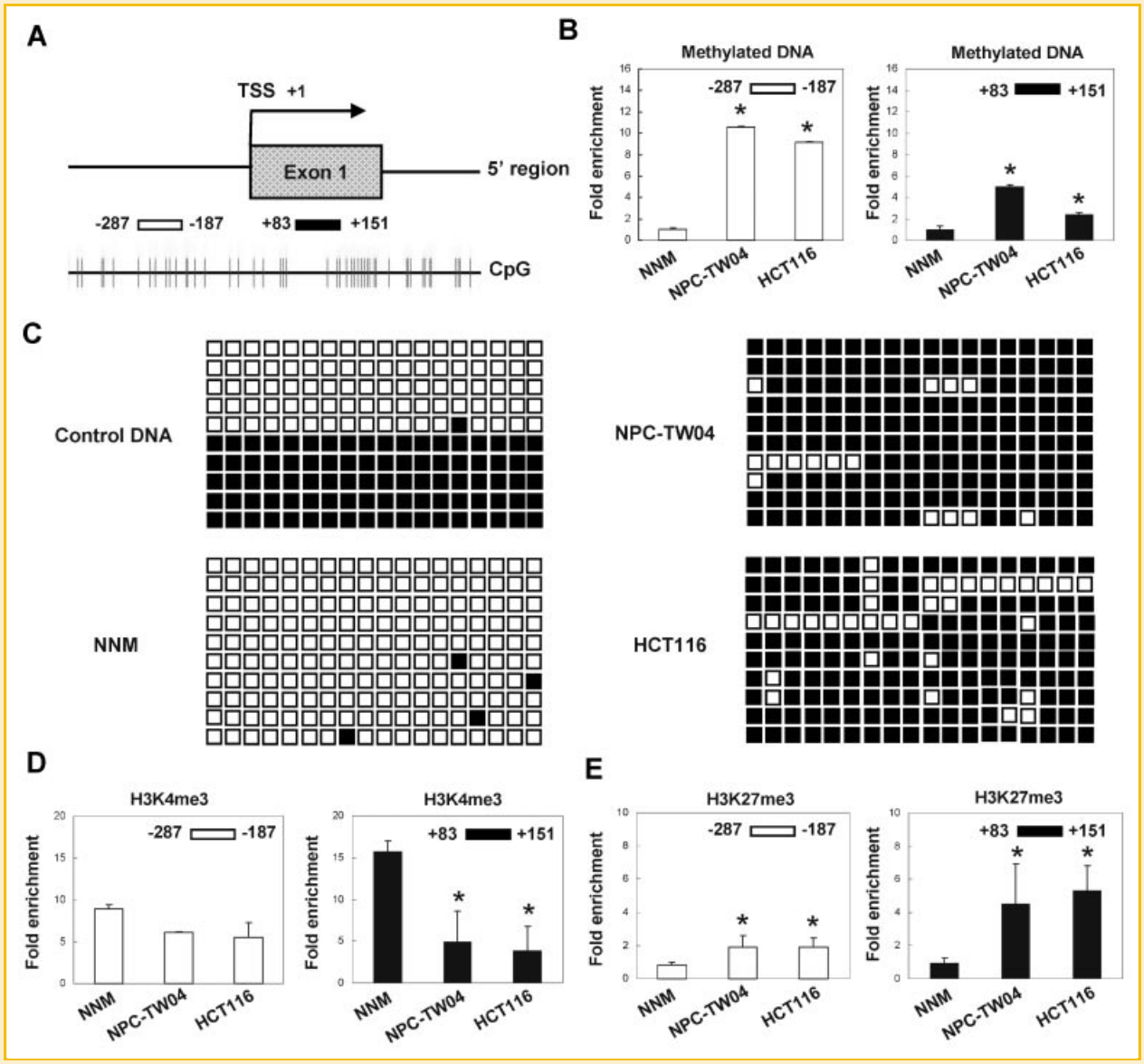

Fig. 5. Methylation status and histone modification associated with OPG promoter in NNM and in NPC-TW04 and HCT116 cancer cells. A: CpG island of the OPG promoter region and primer location for methylation and histone modification analysis (TSS: transcription start site). B: Quantitative analyses of methylated DNA at OPG promoter in NNM, NPC-TW04 and HCT116 cells. The methylation status of NNM cells was designated as 1 ($^{*}P < 0.05$). C: Bisulfite genomic sequencing of individual clones across −386 to −43 of the OPG promoter region. Each square denotes a CpG site across PCR fragments amplified from NNM, NPC-TW04, and HCT116. Filled squares: methylated; open squares: unmethylated. Control DNA was used to evaluate primers property. D: ChIP assays were performed using antibodies against the H3K4me3 modifications and analyzed by quantitative PCR. The relative enrichments (IP/Input) are shown encompassing the indicated promoter regions. The experiment was done in triplicate (mean ± SD). Significant enrichment of H3K4me3 was found in NNM at downstream locus of OPG promoter region. E: Enrichment of H3K27me3 repression mark at both upstream and downstream locus of OPG TSS in NPC-TW04 and HCT116, not in NNM ($^{*}P < 0.05$). [Color figure can be viewed in the online issue, which is available at www.interscience.wiley.com.]

signaling transduced by OPG and its associated functional receptor on the surface of the plasma membrane.

In this study, OPG was shown to be expressed in non-tumor NNP patients, whereas its expression in NPC patient was repressed, though the extent of repression was not consistent (Fig. 4A). This difference may be in part due to individual diversity in the nature of the tumors or the contents of the normal cells within the tumor tissues. Further, we demonstrated OPG expression pattern in tumor tissues by immunohistochemistry using MAb OPG23-1. OPG was detected in the stromal region of tumors but not in cancer cells (Fig. 4B). Down-regulation of OPG in NPC cells was originally identified from our cDNA microarray data. This molecule was found not only to be down-regulated in cancer cells but also to correlate significantly to clinicopathologial findings.

Down-regulation of OPG expression in cancer cells made us interested in studying the regulation mechanism of this gene. Our study demonstrates that two potential epigenetic mechanisms are involved in OPG gene repression in cancer cells. These include DNA

methylation of the OPG promoter and transcriptional repression through chromatin architecture alteration caused by histone modification (Fig. 5). This phenomenon corresponds to a recently proposed histone code hypothesis in which distinct modifications at particular sites of the histone tail compose a histone code causing transcription machinery to interact with histone–DNA complexes [Jenuwein and Allis, 2001]. To gain a better understanding of OPG susceptibility to hypermethylation in cancer, we studied DNA methylation status of OPG promoter by evaluating MeCP2 binding to CpG sites and bisulfite genomic sequencing. We noticed that down-regulation of OPG in cancer cells occurred as a result of enhanced promoter methylation (Fig. 5B,C). Likewise, the epigenetic silencing mark tri-methylation of H3K27 at OPG promoter region was also found to be increased in cancer cells (Fig. 5E). These findings suggest that histone modification may act as a prerequisite for DNA methylation in cohort to cause gene silencing. Contrary to tri-methylation of H3K27, the activation mark tri-methylation of H3K4 was reduced in tumors at OPG promoter region (Fig. 5D). Collectively, these findings demonstrate that abnormal DNA methylation accompanied with aberrant histone lysine methylations may result in chromatin compaction and thus gene silencing.

In conclusion, based on the present experiments, we suggest that the OPG molecule may play potential roles in regulating the progression of cancers. OPG is ubiquitously down-regulated in all NPC cell lines and various cancer cells as well as surgical specimens. Since OPG represses cell proliferation, inactivation of OPG by hypermethylation and chromatin structure alteration may emerge as an important mechanism behind tumor growth. These results suggest that OPG may be a potential tumor suppressor. Further understanding the biology of OPG in cancer may yield new strategies for the diagnosis, prognosis and treatment of cancer.

ACKNOWLEDGMENTS

This work was supported by Academia Sinica (to H-C Wu) and National Science Council, Taiwan (to H-C Wu; NSC-96-2323-B-001-002).

REFERENCES

Ashkenazi A. 2002. Targeting death and decoy receptors of the tumour-necrosis factor superfamily. Nat Rev Cancer 2:420–430.

Barski A, Cuddapah S, Cui K, Roh TY, Schones DE, Wang Z, Wei G, Chepelev I, Zhao K. 2007. High-resolution profiling of histone methylations in the human genome. Cell 129:823–837.

Baylin SB, Ohm JE. 2006. Epigenetic gene silencing in cancer—A mechanism for early oncogenic pathway addiction? Nat Rev Cancer 6:107–116.

Capparelli C, Kostenuik PJ, Morony S, Starnes C, Weimann B, Van G, Scully S, Qi M, Lacey DL, Dunstan CR. 2000. Osteoprotegerin prevents and reverses hypercalcemia in a murine model of humoral hypercalcemia of malignancy. Cancer Res 60:783–787.

Chen YC, Huang HN, Lin CT, Chen YF, King CC, Wu HC. 2007. Generation and characterization of monoclonal antibodies against dengue virus type 1 for epitope mapping and serological detection by epitope-based peptide antigens. Clin Vaccine Immunol 14:404–411.

Chu YW, Yang PC, Yang SC, Shyu YC, Hendrix MJ, Wu R, Wu CW. 1997. Selection of invasive and metastatic subpopulations from a human lung adenocarcinoma cell line. Am J Respir Cell Mol Biol 17:353–360.

Corey E, Brown LG, Kiefer JA, Quinn JE, Pitts TE, Blair JM, Vessella RL. 2005. Osteoprotegerin in prostate cancer bone metastasis. Cancer Res 65:1710–1718.

Corey E, Quinn JE, Bladou F, Brown LG, Roudier MP, Brown JM, Buhler KR, Vessella RL. 2002. Establishment and characterization of osseous prostate cancer models: Intra-tibial injection of human prostate cancer cells. Prostate 52:20–33.

Croucher PI, Shipman CM, Lippitt J, Perry M, Asosingh K, Hijzen A, Brabbs AC, van Beek EJ, Holen I, Skerry TM, Dunstan CR, Russell GR, Van Camp B, Vanderkerken K. 2001. Osteoprotegerin inhibits the development of osteolytic bone disease in multiple myeloma. Blood 98:3534–3540.

Emery JG, McDonnell P, Burke MB, Deen KC, Lyn S, Silverman C, Dul E, Appelbaum ER, Eichman C, DiPrinzio R, Dodds RA, James IE, Rosenberg M, Lee JC, Young PR. 1998. Osteoprotegerin is a receptor for the cytotoxic ligand TRAIL. J Biol Chem 273:14363–14367.

Esteller M. 2007. Cancer epigenomics: DNA methylomes and histone-modification maps. Nat Rev Genet 8:286–298.

Fizazi K, Yang J, Peleg S, Sikes CR, Kreimann EL, Daliani D, Olive M, Raymond KA, Janus TJ, Logothetis CJ, Karsenty G, Navone NM. 2003. Prostate cancer cells-osteoblast interaction shifts expression of growth/survival-related genes in prostate cancer and reduces expression of osteoprotegerin in osteoblasts. Clin Cancer Res 9:2587–2597.

Holen I, Croucher PI, Hamdy FC, Eaton CL. 2002. Osteoprotegerin (OPG) is a survival factor for human prostate cancer cells. Cancer Res 62:1619–1623.

Jenuwein T, Allis CD. 2001. Translating the histone code. Science 293:1074–1080.

Kohler G, Milstein C. 1975. Continuous cultures of fused cells secreting antibody of predefined specificity. Nature 256:495–497.

Kong YY, Yoshida H, Sarosi I, Tan HL, Timms E, Capparelli C, Morony S, Oliveira-dos-Santos AJ, Van G, Itie A, Khoo W, Wakeham A, Dunstan CR, Lacey DL, Mak TW, Boyle WJ, Penninger JM. 1999. OPGL is a key regulator of osteoclastogenesis, lymphocyte development and lymph-node organogenesis. Nature 397:315–323.

Lacey DL, Timms E, Tan HL, Kelley MJ, Dunstan CR, Burgess T, Elliott R, Colombero A, Elliott G, Scully S, Hsu H, Sullivan J, Hawkins N, Davy E, Capparelli C, Eli A, Qian YX, Kaufman S, Sarosi I, Shalhoub V, Senaldi G, Guo J, Delaney J, Boyle WJ. 1998. Osteoprotegerin ligand is a cytokine that regulates osteoclast differentiation and activation. Cell 93:165–176.

Lamoureux F, Richard P, Wittrant Y, Battaglia S, Pilet P, Trichet V, Blanchard F, Gouin F, Pitard B, Heymann D, Redini F. 2007. Therapeutic relevance of osteoprotegerin gene therapy in osteosarcoma: Blockade of the vicious cycle between tumor cell proliferation and bone resorption. Cancer Res 67:7308–7318.

Lee TY, Lin CT, Kuo SY, Chang DK, Wu HC. 2007. Peptide-mediated targeting to tumor blood vessels of lung cancer for drug delivery. Cancer Res 67:10958–10965.

Lin CT, Wong CI, Chan WY, Tzung KW, Ho JK, Hsu MM, Chuang SM. 1990. Establishment and characterization of two nasopharyngeal carcinoma cell lines. Lab Invest 62:713–724.

Lin CT, Chan WY, Chen W, Huang HM, Wu HC, Hsu MM, Chuang SM, Wang CC. 1993. Characterization of seven newly established nasopharyngeal carcinoma cell lines. Lab Invest 68:716–727.

Lin YF, Wu MS, Chang CC, Lin SW, Lin JT, Sun YJ, Chen DS, Chow LP. 2006. Comparative immunoproteomics of identification and characterization of virulence factors from Helicobacter pylori related to gastric cancer. Mol Cell Proteomics 5:1484–1496.

Lo A, Lin CT, Wu HC. 2008. Hepatocellular carcinoma cell-specific peptide ligand for targeted drug delivery. Mol Cancer Ther 7:579–589.

Martin C, Zhang Y. 2005. The diverse functions of histone lysine methylation. Nat Rev Mol Cell Biol 6:838–849.

Meehan RR, Lewis JD, Bird AP. 1992. Characterization of MeCP2, a vertebrate DNA binding protein with affinity for methylated DNA. Nucleic Acids Res 20:5085–5092.

Pearse RN, Sordillo EM, Yaccoby S, Wong BR, Liau DF, Colman N, Michaeli J, Epstein J, Choi Y. 2001. Multiple myeloma disrupts the TRANCE/ osteoprotegerin cytokine axis to trigger bone destruction and promote tumor progression. Proc Natl Acad Sci USA 98:11581–11586.

Secchiero P, Corallini F, Pandolfi A, Consoli A, Candido R, Fabris B, Celeghini C, Capitani S, Zauli G. 2006. An increased osteoprotegerin serum release characterizes the early onset of diabetes mellitus and may contribute to endothelial cell dysfunction. Am J Pathol 169:2236–2244.

Shipman CM, Croucher PI. 2003. Osteoprotegerin is a soluble decoy receptor for tumor necrosis factor-related apoptosis-inducing ligand/Apo2 ligand and can function as a paracrine survival factor for human myeloma cells. Cancer Res 63:912–916.

Simonet WS, Lacey DL, Dunstan CR, Kelley M, Chang MS, Luthy R, Nguyen HQ, Wooden S, Bennett L, Boone T, Shimamoto G, DeRose M, Elliott R, Colombero A, Tan HL, Trail G, Sullivan J, Davy E, Bucay N, Renshaw-Gegg L, Hughes TM, Hill D, Pattison W, Campbell P, Sander S, Van G, Tarpley J, Derby P, Lee R, Boyle WJ. 1997. Osteoprotegerin: A novel secreted protein involved in the regulation of bone density. Cell 89:309–319.

Strathdee CA, McLeod MR, Hall JR. 1999. Efficient control of tetracycline-responsive gene expression from an autoregulated bi-directional expression vector. Gene 229:21–29.

Vanderkerken K, De Leenheer E, Shipman C, Asosingh K, Willems A, Van Camp B, Croucher P. 2003. Recombinant osteoprotegerin decreases tumor burden and increases survival in a murine model of multiple myeloma. Cancer Res 63:287–289.

Wu HC, Jung MY, Chiu CY, Chao TT, Lai SC, Jan JT, Shaio MF. 2003. Identification of a dengue virus type 2 (DEN-2) serotype-specific B-cell epitope and detection of DEN-2-immunized animal serum samples using an epitope-based peptide antigen. J Gen Virol 84:2771–2779.

Yamaguchi K, Kinosaki M, Goto M, Kobayashi F, Tsuda E, Morinaga T, Higashio K. 1998. Characterization of structural domains of human osteoclastogenesis inhibitory factor. J Biol Chem 273:5117–5123.

Yasuda H, Shima N, Nakagawa N, Yamaguchi K, Kinosaki M, Mochizuki S, Tomoyasu A, Yano K, Goto M, Murakami A, Tsuda E, Morinaga T, Higashio K, Udagawa N, Takahashi N, Suda T. 1998. Osteoclast differentiation factor is a ligand for osteoprotegerin/osteoclastogenesis-inhibitory factor and is identical to TRANCE/RANKL. Proc Natl Acad Sci USA 95:3597–3602.

Yonou H, Kanomata N, Goya M, Kamijo T, Yokose T, Hasebe T, Nagai K, Hatano T, Ogawa Y, Ochiai A. 2003. Osteoprotegerin/osteoclastogenesis inhibitory factor decreases human prostate cancer burden in human adult bone implanted into nonobese diabetic/severe combined immunodeficient mice. Cancer Res 63:2096–2102.

Zhang J, Dai J, Qi Y, Lin DL, Smith P, Strayhorn C, Mizokami A, Fu Z, Westman J, Keller ET. 2001. Osteoprotegerin inhibits prostate cancer-induced osteoclastogenesis and prevents prostate tumor growth in the bone. J Clin Invest 107:1235–1244.